

## Article

# A New Method for Displacement Modelling of Serial Robots Using Finite Screw

Feiyang Xue<sup>1</sup>, Zhengjun Fang<sup>1</sup>, Jiahao Song<sup>1</sup>, Qi Liu<sup>2</sup> and Shuofei Yang<sup>1,\*</sup> 

<sup>1</sup> College of Engineering, China Agricultural University, Beijing 100083, China; feiyang.xue@cau.edu.cn (F.X.); fang\_zhengjun@cau.edu.cn (Z.F.); jiahao.song@cau.edu.cn (J.S.)

<sup>2</sup> Tianjin Key Laboratory for Advanced Mechatronic System Design and Intelligent Control, School of Mechanical Engineering, Tianjin University of Technology, Tianjin 300384, China; rufei67@163.com

\* Correspondence: shuofei.yang@cau.edu.cn

**Abstract:** Kinematics is a hot topic in robotic research, serving as a foundational step in the synthesis and analysis of robots. Forward kinematics and inverse kinematics are the prerequisite and foundation for motion control, trajectory planning, dynamic simulation, and precision guarantee of robotic manipulators. Both of them depend on the displacement models. Compared with the previous work, finite screw is proven to be the simplest and nonredundant mathematical tool for displacement description. Thus, it is used for displacement modelling of serial robots in this paper. Firstly, a finite-screw-based method for formulating displacement model is proposed, which is applicable for any serial robot. Secondly, the procedures for forward and inverse kinematics by solving the formulated displacement equation are discussed. Then, two typical serial robots with three translations and two rotations are taken as examples to illustrate the proposed method. Finally, through Matlab simulation, the obtained analytical expressions of kinematics are verified. The main contribution of the proposed method is that finite-screw-based displacement model is highly related with instantaneous-screw-based kinematic and dynamic models, providing an integrated modelling and analysis methodology for robotic mechanisms.

**Keywords:** displacement modelling; kinematics; serial robots; finite screw; screw theory



**Citation:** Xue, F.; Fang, Z.; Song, J.; Liu, Q.; Yang, S. A New Method for Displacement Modelling of Serial Robots Using Finite Screw. *Machines* **2024**, *12*, 658. <https://doi.org/10.3390/machines12090658>

Academic Editor: Huosheng Hu

Received: 8 August 2024

Revised: 4 September 2024

Accepted: 14 September 2024

Published: 20 September 2024



**Copyright:** © 2024 by the authors. Licensee MDPI, Basel, Switzerland. This article is an open access article distributed under the terms and conditions of the Creative Commons Attribution (CC BY) license (<https://creativecommons.org/licenses/by/4.0/>).

## 1. Introduction

Robots have been widely utilized in industrial application in recent years [1,2]. Kinematics, including forward kinematics and inverse kinematics, is a fundamental problem in the synthesis and analysis of robots. It is the prerequisite for motion control, trajectory planning, dynamic simulation, and precision guarantee of robotic manipulators. Both forward kinematics and inverse kinematics depend on displacement modelling. Through describing displacements of robots by mathematical tools, displacement models can be formulated in an algebraic way [3–5]. The two main issues involved in displacement modelling of robots are as follows:

- (1) Select a mathematical tool to analytically express the displacements generated by the joints of the robots [6];
- (2) Formulate the displacement equations of the robots by compositing the joints' displacements [7].

Up to now, two main kinds of methods for displacement modelling of serial robots (SRs) have been proposed, i.e., vector chain methods and product of exponentials methods. In vector chain methods, three-dimensional position vectors are employed to formulate the displacement equation by means of building mappings between positions and orientations of the end-effector of an SR at the given pose [8]. In the formulated position equations, all joint parameters are independent and decoupled. In the product of exponentials method, exponential matrices (or dual quaternions) containing joint parameters are used to express

pose transformations between adjacent links of an SR [9]. The displacement equation can be formulated by multiplying these matrices or (or dual quaternions) together [10,11].

By employing these methods, displacement models of any SR can be formulated. Forward kinematics can be directly carried out by applying the obtained displacement equation [12]. Additionally, some methods for inverse kinematics have also been put forward, which accompany the displacement modelling methods. The works related to vector chain methods have been reported by elimination and engine value analysis of univariate polynomial equations [13]. The works related to the product of exponentials methods can be found by algebraic and geometric approaches [14].

Compared with the mathematical tools used in these existing methods, finite screw has the following advantages in describing displacements of serial robots and their joints:

(1) It has only six items, which is the simplest and nonredundant description of the special Euclidean group (SE(3)) [15].

(2) The algebraic structure of the entire set of finite screws has been proved to be a Lie group under the screw triangle product, while the entire set of instantaneous screw is its corresponding Lie algebra [16].

Considering that the instantaneous screw and its isomorphism have been successfully and widely used in mobility, velocity, dynamic, accuracy, and stiffness modelling of SRs [17–20], we intend to use the counterpart of it, i.e., finite screw, in implementing displacement modelling. Based upon Dai's works [21–23], finite screw will be used in displacement modelling of SRs in this paper.

The contributions of this paper lie in the following points.

(1) Displacement modelling based upon finite screw formulates the nonredundant and most concise expression for forward and inverse kinematics of SRs [24,25].

(2) The computational cost of displacement modelling is improved by introducing finite screw and the corresponding algorithms of screw triangle product [26].

(3) The formulated displacement models of SRs are highly related with the velocity and higher kinematic models because of the differential mapping between finite and instantaneous screws, providing integrated method for kinematics and dynamics modelling [27,28].

This paper presents a new method for displacement modelling of SRs using finite screws as the mathematical tool, making it applicable to any SR. The organization of this paper is as follows. After a brief review of the state-of-the-art of the existing methods for displacement modelling and kinematics in Section 1, Section 2 presents a new method to algebraically formulate displacement equation of an SR through describing displacements generated by an SR and its joints as finite screws. Then, the procedures of forward and inverse kinematics using the formulated finite-screw-based displacement model are given in Section 3. In Section 4, two topical serial robots are taken as examples to illustrate the proposed method, which is followed by the verification of the correctness of the obtained analytical expressions in Matlab simulation in Section 5. The conclusions are drawn in Section 6.

## 2. Displacement Modelling Using Finite Screw

In this section, the displacement equation will be formulated through describing displacements generated by an SR and its joints by finite screws, which clearly shows the algebraic mappings between all the joint parameters and the pose of the end-effector [29].

In Chasles' theorem, a rigid body displacement from one configuration to another configuration can always be regarded as the rigid body rotating around an axis together with translating along the axis. The axis is called Chasles' axis. As is well known, for the Chasles' axis, the rotational angle and translational distance about/along that axis are the basic elements of displacement [30,31]. Among all the mathematical tools used to describe displacement, the finite screw in quasi-vector form can clearly express these basic elements in the simplest and most nonredundant manner, which can be analytically

composed [32,33]. Generally, a displacement of a rigid body can be expressed by a finite screw as follows:

$$S_f = 2 \tan \frac{\theta}{2} \begin{pmatrix} s_f \\ r_f \times s_f \end{pmatrix} + \tau \begin{pmatrix} \mathbf{0} \\ s_f \end{pmatrix}, \quad (1)$$

where  $s_f$  ( $|s_f| = 1$ ) and  $r_f$  denote the unit direction vector and position vector of the Chasles' axis,  $(s_f; r_f \times s_f)$  is the Plücker coordinates of the screw axis of the displacement, and  $\theta$  and  $\tau$  are the rotational angle and translational distance about/along that axis [34,35].

Suppose that a rigid body realizes two successive displacements expressed by

$$S_{f,i} = 2 \tan \frac{\theta_i}{2} \begin{pmatrix} s_{f,i} \\ r_{f,i} \times s_{f,i} \end{pmatrix} + \tau_i \begin{pmatrix} \mathbf{0} \\ s_{f,i} \end{pmatrix}, \quad i = a, b. \quad (2)$$

The screw triangle product [23] is the composition algorithm of finite screws. The composition of two finite screws results in the linear addition of these two screws, the screw along their common perpendicular, and their translational parts. The resultant displacement of this rigid body can be obtained by compositing the two finite screws using the screw triangle product,

$$S_{f,ab} = S_{f,a} \bar{\circ} S_{f,b} = \frac{S_{f,a} + S_{f,b} + \frac{S_{f,b} \times S_{f,a}}{2} - \tan \frac{\theta_a}{2} \tan \frac{\theta_b}{2} \left( \tau_b \begin{pmatrix} \mathbf{0} \\ s_{f,a} \end{pmatrix} + \tau_a \begin{pmatrix} \mathbf{0} \\ s_{f,b} \end{pmatrix} \right)}{1 - \tan \frac{\theta_a}{2} \tan \frac{\theta_b}{2} s_{f,a}^T s_{f,b}}, \quad (3)$$

where the symbol " $\bar{\circ}$ " is used to denote the screw triangle product.

By employing finite screws to describe the displacements generated by an SR and its joints, the displacement model of the robot can be directly formulated utilizing screw triangle products [36,37]. In this way, for an SR constituted by  $n$  one-DoF joints (revolute (R) and prismatic (P) joints), its displacement model can be obtained as follows using Equations (1) and (3),

$$S_{f,SR} = S_{f,n} \bar{\circ} S_{f,n-1} \bar{\circ} \cdots \bar{\circ} S_{f,1}, \quad (4)$$

where  $S_{f,SR}$  and  $S_{f,k}$  ( $k = 1, 2, \dots, n$ ) denote the displacements generated by the SR and its  $k$ th joint measured from a preset initial pose. According to Equation (1),  $S_{f,k}$  can be expressed as follows:

$$S_{f,k} = \begin{cases} 2 \tan \frac{\theta_k}{2} \begin{pmatrix} s_k \\ r_k \times s_k \end{pmatrix} & \text{R joint} \\ \tau_k \begin{pmatrix} \mathbf{0} \\ s_k \end{pmatrix} & \text{P joint} \end{cases} \quad (5)$$

where  $s_k$  and  $r_k$  are the unit direction vector and position vector of the  $k$ th joint at its initial pose;  $\theta_k$  ( $\tau_k$ ) is the rotational angle (translational distance) of the  $k$ th joint with respect to its initial pose [38,39]. Conventionally, joints in the SR are numbered from the fixed base to the end-effector. Equation (4) is the finite-screw-based displacement model (displacement equation) of the SR [40,41].

### 3. Kinematics Using Finite Screw

Having the finite-screw-based displacement equation at hand, the kinematics of SRs can be carried out [42,43]. The procedures for forward and inverse kinematics by utilizing this displacement equation will be discussed in this section.

According to Chasles' theorem and screw triangle product, the composition of several joint displacements can always be rewritten as a finite screw [44–46]. Hence, the displacement model of SR can be rewritten into the following form:

$$S_{f,SR} = S_{f,n} \bar{\circ} S_{f,n-1} \bar{\circ} \cdots \bar{\circ} S_{f,1} = 2 \tan \frac{\theta_C}{2} \begin{pmatrix} s_C \\ r_C \times s_C \end{pmatrix} + \tau_C \begin{pmatrix} \mathbf{0} \\ s_C \end{pmatrix}, \quad (6)$$

where  $s_C$  and  $r_C$  are unit direction vector and position vector of the axis of the composition displacement, and  $\theta_C$  and  $\tau_C$  are rotational angle and translational distance about and along that axis [47,48]. It is easy to see that they are all functions of the joint parameters  $\theta_k$  and  $\tau_k$  ( $k = 1, 2, \dots, n$ ) as

$$\begin{aligned} s_C &= f_s(\theta_1, \theta_2, \dots, \theta_n), \quad r_C = f_r(\theta_1/\tau_1, \theta_2/\tau_2, \dots, \theta_n/\tau_n), \\ \tan \frac{\theta_C}{2} &= f_\theta(\theta_1, \theta_2, \dots, \theta_n), \quad \tau_C = f_t(\theta_1/\tau_1, \theta_2/\tau_2, \dots, \theta_n/\tau_n). \end{aligned} \quad (7)$$

We write the current pose of the SR's end-effector as

$$S_{f,SR} = 2 \tan \frac{\theta_{SR}}{2} \begin{pmatrix} s_{SR} \\ r_{SR} \times s_{SR} \end{pmatrix} + \tau_{SR} \begin{pmatrix} 0 \\ s_{SR} \end{pmatrix}. \quad (8)$$

Because the composition displacement generated by all the joints is equivalent to the pose of the end-effector [49–51], Equation (6) can be rewritten into the following three mappings between the joint parameters and the end-effector pose,

$$s_{SR} = f_s(\theta_1, \theta_2, \dots, \theta_n), \quad (9)$$

$$\tan \frac{\theta_{SR}}{2} = f_\theta(\theta_1, \theta_2, \dots, \theta_n), \quad (10)$$

$$\begin{aligned} &2 \tan \frac{\theta_{SR}}{2} r_{SR} \times s_{SR} + \tau_{SR} s_{SR} \\ &= 2 f_\theta(\theta_1, \theta_2, \dots, \theta_n) \cdot (f_r(\theta_1/\tau_1, \theta_2/\tau_2, \dots, \theta_n/\tau_n) \times f_s(\theta_1, \theta_2, \dots, \theta_n)) \\ &+ f_t(\theta_1/\tau_1, \theta_2/\tau_2, \dots, \theta_n/\tau_n) \cdot f_s(\theta_1, \theta_2, \dots, \theta_n) \\ &= g(\theta_1/\tau_1, \theta_2/\tau_2, \dots, \theta_n/\tau_n) \end{aligned} \quad (11)$$

In the above three equations,  $f_s$  and  $f_\theta$  are the mappings between the rotational parameters of joints and the end-effector orientation, and  $g$  is the mapping between the joint parameters and the end-effector position [52–54]. They clearly reveal the algebraic mappings between the joint parameters and the end-effector pose [55–57]. In these mappings,  $s_k$  and  $r_k$  are determined by the preset initial pose of the SR. They are known quantities, which are invariable with the pose that the end-effector moves to [58–60]. In forward kinematics, the  $n$  joint parameters,  $\theta_1/\tau_1, \theta_2/\tau_2, \dots, \theta_n/\tau_n$ , are given, and the displacement  $S_{f,SR}$  generated by the SR with respect to the initial pose, i.e., the current pose of the end-effector, is what needs to be solved. In inverse kinematics, the displacement of the SR is given, and the  $n$  joint parameters are the variables needed to be solved. It is noted that the symbol “/” here means “or”, because only one of  $\theta_k$  and  $\tau_k$  exists [61–63].

From the above analysis, the procedures for forward and inverse kinematics utilizing finite screw can be concluded as follows:

- (1) Formulate the displacement model of an SR using the finite screws generated by its joints [64,65].
- (2) Rewrite the displacement equation into the mappings between the joint parameters of the end-effector pose [66].
- (3) Given the joint parameters, the forward kinematics leads to the end-effector pose [67,68].
- (4) Given the end-effector pose, the inverse kinematics results in the joint parameters [69,70].

The procedures for forward and inverse kinematics are illustrated in Figure 1.

Through vector and polynomial analysis, the analytical solutions of forward and inverse kinematics can be derived by following the procedures [71,72]. In the next section, two topical SRs will be taken as examples to show the validity of the proposed finite screw method.

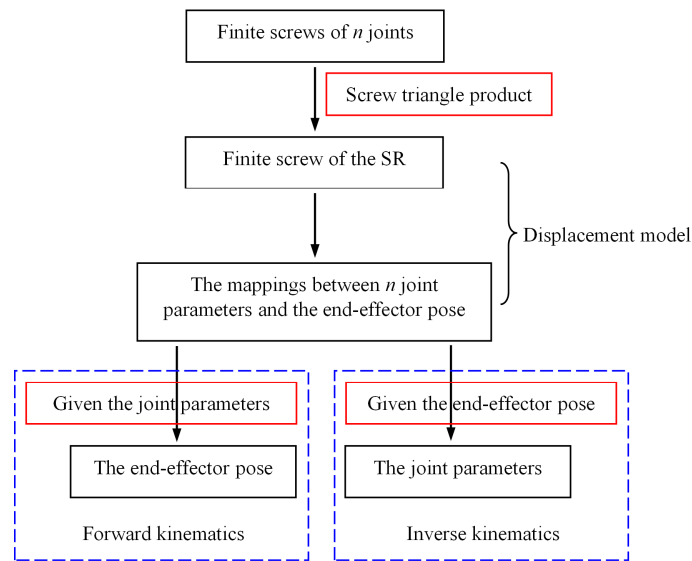


Figure 1. The procedures for forward and inverse kinematics.

4. Examples

The method and procedures proposed in this paper can be applied to displacement modelling and kinematics of SRs. In this section,  $P_1P_2P_3R_aR_b$  and  $R_aR_aR_aR_bR_b$  robots with three translations and two rotations are taken as typical examples to illustrate the method. In order to show the procedures more clearly, we firstly solve the  $P_1P_2P_3R_aR_b$  robot, and then use the result to solve  $R_aR_aR_aR_bR_b$ . Here, the subscript of each R or P joint denotes its direction.

4.1.  $P_1P_2P_3R_aR_b$  Robot

As shown in Figure 2,  $P_1P_2P_3R_aR_b$  is the three-translational and two-rotational robot with the simplest structure. It generates two rotations with fixed directions. Its displacement equation can be formulated based upon Equation (4),

$$S_{f,SR} = 2 \tan \frac{\theta_b}{2} \begin{pmatrix} s_b \\ r_b \times s_b \end{pmatrix} \circ 2 \tan \frac{\theta_a}{2} \begin{pmatrix} s_a \\ r_a \times s_a \end{pmatrix} \circ \tau_3 \begin{pmatrix} 0 \\ s_3 \end{pmatrix} \circ \tau_2 \begin{pmatrix} 0 \\ s_2 \end{pmatrix} \circ \tau_1 \begin{pmatrix} 0 \\ s_1 \end{pmatrix}, \quad (12)$$

where  $s_a$  and  $s_b$ , respectively, denote the unit direction vectors of  $R_a$  and  $R_b$ ,  $r_a$  and  $r_b$  denote the position vectors of the two R joints,  $\theta_a$  and  $\theta_b$  denote their rotational angles,  $s_1$ ,  $s_2$ , and  $s_3$  are the unit vectors of  $P_1$ ,  $P_2$ , and  $P_3$ , and  $\tau_1$ ,  $\tau_2$ , and  $\tau_3$  are their translational distances.

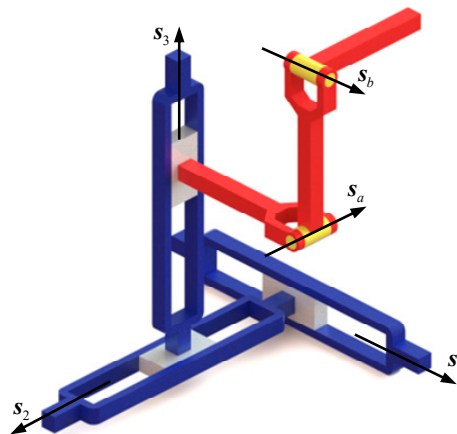


Figure 2.  $P_1P_2P_3R_aR_b$  robot.

Computing the composition displacements generated by all joints in  $P_1P_2P_3R_aR_b$ , Equation (12) can be rewritten as follows by utilizing the screw triangle product,

$$2 \tan \frac{\theta_{SR}}{2} \left( \mathbf{r}_{SR} \times \mathbf{s}_{SR} + \frac{t_{SR}}{2 \tan \frac{\theta_{SR}}{2}} \mathbf{s}_{SR} \right) = 2 \tan \frac{\theta_C}{2} \left( \mathbf{p}_{ba} + \frac{\mathbf{s}_C}{2} + \frac{t}{2 \tan \frac{\theta_C}{2}} \right), \quad (13)$$

where

$$\begin{aligned} \tan \frac{\theta_{SR}}{2} &= \tan \frac{\theta_C}{2} = \frac{\left| \tan \frac{\theta_a}{2} \mathbf{s}_a + \tan \frac{\theta_b}{2} \mathbf{s}_b + \tan \frac{\theta_a}{2} \tan \frac{\theta_b}{2} (\mathbf{s}_a \times \mathbf{s}_b) \right|}{1 - \tan \frac{\theta_a}{2} \tan \frac{\theta_b}{2} \mathbf{s}_a^T \mathbf{s}_b}, \\ \mathbf{s}_{SR} &= \mathbf{s}_C = \frac{\tan \frac{\theta_a}{2} \mathbf{s}_a + \tan \frac{\theta_b}{2} \mathbf{s}_b + \tan \frac{\theta_a}{2} \tan \frac{\theta_b}{2} (\mathbf{s}_a \times \mathbf{s}_b)}{\left| \tan \frac{\theta_a}{2} \mathbf{s}_a + \tan \frac{\theta_b}{2} \mathbf{s}_b + \tan \frac{\theta_a}{2} \tan \frac{\theta_b}{2} (\mathbf{s}_a \times \mathbf{s}_b) \right|}, \\ \mathbf{p}_{ba} &= \frac{\tan \frac{\theta_a}{2} (\mathbf{r}_a \times \mathbf{s}_a) + \tan \frac{\theta_b}{2} (\mathbf{r}_b \times \mathbf{s}_b) + \tan \frac{\theta_a}{2} \tan \frac{\theta_b}{2} (\mathbf{s}_a \times (\mathbf{r}_b \times \mathbf{s}_b)) + (\mathbf{r}_a \times \mathbf{s}_a) \times \mathbf{s}_b}{\left| \tan \frac{\theta_a}{2} \mathbf{s}_a + \tan \frac{\theta_b}{2} \mathbf{s}_b + \tan \frac{\theta_a}{2} \tan \frac{\theta_b}{2} (\mathbf{s}_a \times \mathbf{s}_b) \right|}, \\ t &= \tau_1 \mathbf{s}_1 + \tau_2 \mathbf{s}_2 + \tau_3 \mathbf{s}_3 \end{aligned}$$

Using these equations, the forward kinematics can be derived in a straightforward way, when the joint parameters are given.

When the end-effector pose is given, the two rotational parameters,  $\theta_a$  and  $\theta_b$ , can be analytically solved through vector analysis,

$$\theta_a = 2 \arctan \left( \frac{\mathbf{s}_{SR}^T (\mathbf{s}_a \times \mathbf{s}_b)}{\mathbf{s}_{SR}^T \mathbf{s}_b - \mathbf{s}_a^T \mathbf{s}_b \mathbf{s}_{SR}^T \mathbf{s}_a} \right), \quad \theta_b = 2 \arctan \left( \frac{\mathbf{s}_{SR}^T (\mathbf{s}_a \times \mathbf{s}_b)}{\mathbf{s}_{SR}^T \mathbf{s}_a - \mathbf{s}_a^T \mathbf{s}_b \mathbf{s}_{SR}^T \mathbf{s}_b} \right). \quad (14)$$

In order to solve the three P joint parameters,  $\tau_1$ ,  $\tau_2$ , and  $\tau_3$ , the mapping between these three parameters and the given position is built as

$$\mathbf{t} = \left( \frac{\mathbf{E}_3}{2 \tan \frac{\theta_C}{2}} - \frac{\tilde{\mathbf{s}}_C}{2} \right)^{-1} \left( \mathbf{r}_{SR} \times \mathbf{s}_{SR} + \frac{\tau_{SR}}{2 \tan \frac{\theta_{SR}}{2}} \mathbf{s}_{SR} - \mathbf{p}_{ba} \right). \quad (15)$$

where  $\tilde{\mathbf{s}}_{ba}$  denotes the skew-symmetric matrix of  $\mathbf{s}_{ba}$ , and  $\mathbf{E}_3$  is a unit matrix of order three.

Computing the projections of the translation vector  $\mathbf{t}$  on directions of  $\mathbf{s}_1$ ,  $\mathbf{s}_2$ , and  $\mathbf{s}_3$  leads to the parameters  $\tau_1$ ,  $\tau_2$ , and  $\tau_3$ ,

$$\tau_1 = \frac{\mathbf{t}^T (\mathbf{s}_2 \times \mathbf{s}_3)}{\mathbf{s}_1^T (\mathbf{s}_2 \times \mathbf{s}_3)}, \quad \tau_2 = \frac{\mathbf{t}^T (\mathbf{s}_1 \times \mathbf{s}_3)}{\mathbf{s}_2^T (\mathbf{s}_1 \times \mathbf{s}_3)}, \quad \tau_3 = \frac{\mathbf{t}^T (\mathbf{s}_1 \times \mathbf{s}_2)}{\mathbf{s}_3^T (\mathbf{s}_1 \times \mathbf{s}_2)}. \quad (16)$$

In fact, the displacement equation of any three-translational and two-rotational SR with two fixed rotation directions can be rewritten into a form that is similar to Equation (13). Thus, its two rotational parameters can be obtained using the mapping built in the similar way. The differences between solving different three-translational and two-rotational SRs come from the diversification mappings between the three translational parameters and the given position of end-effectors. Hence, forward and inverse kinematics of the  $R_aR_aR_aR_bR_b$  robot can be solved as follows.

#### 4.2. $R_aR_aR_aR_bR_b$ Robot

The  $R_aR_aR_aR_bR_b$  robot in Figure 3 consists of three  $R_a$  and two  $R_b$  joints, and its displacement equation can be formulated as

$$\begin{aligned} \mathbf{S}_{f,SR} &= 2 \tan \frac{\theta_{b2}}{2} \begin{pmatrix} \mathbf{s}_b \\ \mathbf{r}_{b2} \times \mathbf{s}_b \end{pmatrix} \circledast 2 \tan \frac{\theta_{b1}}{2} \begin{pmatrix} \mathbf{s}_b \\ \mathbf{r}_{b1} \times \mathbf{s}_b \end{pmatrix} \circledast \\ &2 \tan \frac{\theta_{a3}}{2} \begin{pmatrix} \mathbf{s}_a \\ \mathbf{r}_{a3} \times \mathbf{s}_a \end{pmatrix} \circledast 2 \tan \frac{\theta_{a2}}{2} \begin{pmatrix} \mathbf{s}_a \\ \mathbf{r}_{a2} \times \mathbf{s}_a \end{pmatrix} \circledast 2 \tan \frac{\theta_{a1}}{2} \begin{pmatrix} \mathbf{s}_a \\ \mathbf{r}_{a1} \times \mathbf{s}_a \end{pmatrix} \end{aligned} \quad (17)$$

where  $r_{a_1}$ ,  $r_{a_2}$ , and  $r_{a_3}$  denote the position vectors of the three  $R_a$ ,  $\theta_{a_1}$ ,  $\theta_{a_2}$ , and  $\theta_{a_3}$  denote their rotational angles,  $r_{b_1}$  and  $r_{b_2}$  are the position vectors of the two  $R_b$ , and  $\theta_{b_1}$  and  $\theta_{b_2}$  are their rotational angles. The subscripts of the position vectors and rotational angles of the  $R_a$  and  $R_b$  joints are, respectively, numbered from the joint near the fixed base to the joint near the end-effector.

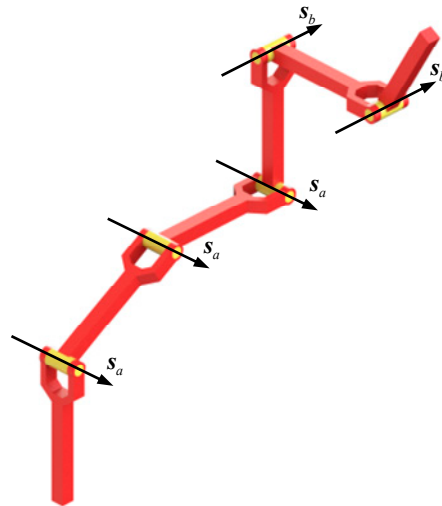


Figure 3.  $R_a R_a R_a R_b R_b$  robot.

Equation (17) can be rewritten as

$$2 \tan \frac{\theta_{SR}}{2} \left( r_{SR} \times s_{SR} + \frac{s_{SR}}{2 \tan \frac{\theta_{SR}}{2}} s_{SR} \right) = 2 \tan \frac{\theta_C}{2} \left( p_{ba} + \frac{s_C}{2} + \frac{t}{2 \tan \frac{\theta_C}{2}} \right) \quad (18)$$

where

$$\tan \frac{\theta_{SR}}{2} = \tan \frac{\theta_C}{2} = \frac{\left| \tan \frac{\theta_{a_1} + \theta_{a_2} + \theta_{a_3}}{2} s_a + \tan \frac{\theta_{b_1} + \theta_{b_2}}{2} s_b + \tan \frac{\theta_{a_1} + \theta_{a_2} + \theta_{a_3}}{2} \tan \frac{\theta_{b_1} + \theta_{b_2}}{2} (s_a \times s_b) \right|}{1 - \tan \frac{\theta_{a_1} + \theta_{a_2} + \theta_{a_3}}{2} \tan \frac{\theta_{b_1} + \theta_{b_2}}{2} s_a^T s_b}$$

$$s_{SR} = s_C = \frac{\tan \frac{\theta_{a_1} + \theta_{a_2} + \theta_{a_3}}{2} s_a + \tan \frac{\theta_{b_1} + \theta_{b_2}}{2} s_b + \tan \frac{\theta_{a_1} + \theta_{a_2} + \theta_{a_3}}{2} \tan \frac{\theta_{b_1} + \theta_{b_2}}{2} (s_a \times s_b)}{\left| \tan \frac{\theta_{a_1} + \theta_{a_2} + \theta_{a_3}}{2} s_a + \tan \frac{\theta_{b_1} + \theta_{b_2}}{2} s_b + \tan \frac{\theta_{a_1} + \theta_{a_2} + \theta_{a_3}}{2} \tan \frac{\theta_{b_1} + \theta_{b_2}}{2} (s_a \times s_b) \right|}$$

$$p_{ba} = \frac{\tan \frac{\theta_{a_1} + \theta_{a_2} + \theta_{a_3}}{2} (r_{a_3} \times s_a) + \tan \frac{\theta_{b_1} + \theta_{b_2}}{2} (r_{b_2} \times s_b) + \tan \frac{\theta_{a_1} + \theta_{a_2} + \theta_{a_3}}{2} \tan \frac{\theta_{b_1} + \theta_{b_2}}{2} (s_a \times (r_{b_2} \times s_b) + (r_{a_3} \times s_a) \times s_b)}{\left| \tan \frac{\theta_{a_1} + \theta_{a_2} + \theta_{a_3}}{2} s_a + \tan \frac{\theta_{b_1} + \theta_{b_2}}{2} s_b + \tan \frac{\theta_{a_1} + \theta_{a_2} + \theta_{a_3}}{2} \tan \frac{\theta_{b_1} + \theta_{b_2}}{2} (s_a \times s_b) \right|}$$

$$t = (\exp((\theta_{a_1} + \theta_{a_2})\tilde{s}_a) - E_3)(r_{a_3} - r_{a_2}) + (\exp(\theta_{a_1}\tilde{s}_a) - E_3)(r_{a_2} - r_{a_1}) + \exp((\theta_{a_1} + \theta_{a_2} + \theta_{a_3})\tilde{s}_a)(\exp(\theta_{b_1}\tilde{s}_b) - E_3)(r_{b_2} - r_{b_1})$$

Similarly, the forward kinematics can be derived in a straightforward way using these equations when the joint parameters are given.

When the end-effector pose is given, the inverse kinematics of this robot is solved as follows. It is easy to see from the expression of  $s_C$  that the two rotations of the SR are, respectively, generated by the three  $R_a$  and the two  $R_b$ . Thus,  $\theta_{a_1} + \theta_{a_2} + \theta_{a_3}$  and  $\theta_{b_1} + \theta_{b_2}$  can be regarded to be the two rotational parameters. From the expression of  $t$ , it can be seen that the three translations are, respectively, generated by the first two  $R_a$ , the first  $R_a$ , and the first  $R_b$ . In this way,  $\theta_{a_1} + \theta_{a_2}$ ,  $\theta_{a_1}$ , and  $\theta_{b_1}$  are the three translational parameters.

The two rotational parameters  $\theta_{a_1} + \theta_{a_2} + \theta_{a_3}$  and  $\theta_{b_1} + \theta_{b_2}$  can be solved in the similar way as shown in Equation (14). The solutions are

$$\begin{aligned}\theta_{a_1} + \theta_{a_2} + \theta_{a_3} &= 2\arctan\left(\frac{\mathbf{s}_{SR}^T(\mathbf{s}_a \times \mathbf{s}_b)}{\mathbf{s}_{SR}^T \mathbf{s}_b - \mathbf{s}_a^T \mathbf{s}_b \mathbf{s}_{SR}^T \mathbf{s}_a}\right), \\ \theta_{b_1} + \theta_{b_2} &= 2\arctan\left(\frac{\mathbf{s}_{SR}^T(\mathbf{s}_a \times \mathbf{s}_b)}{\mathbf{s}_{SR}^T \mathbf{s}_a - \mathbf{s}_a^T \mathbf{s}_b \mathbf{s}_{SR}^T \mathbf{s}_b}\right).\end{aligned}\quad (19)$$

Thus,  $\mathbf{t}$  can be obtained like Equation (15). Using Equation (18), the mapping between  $\mathbf{t}$  and the three translational parameters  $\theta_{a_1} + \theta_{a_2}$ ,  $\theta_{a_1}$ , and  $\theta_{b_1}$  can be obtained as

$$\begin{aligned}&\exp((\theta_{a_1} + \theta_{a_2})\tilde{\mathbf{s}}_a)(\mathbf{r}_{a_3} - \mathbf{r}_{a_2}) + \exp(\theta_{a_1}\tilde{\mathbf{s}}_a)(\mathbf{r}_{a_2} - \mathbf{r}_{a_1}) \\ &+ \exp((\theta_{a_1} + \theta_{a_2} + \theta_{a_3})\tilde{\mathbf{s}}_a)\exp(\theta_{b_1}\tilde{\mathbf{s}}_b)(\mathbf{r}_{b_2} - \mathbf{r}_{b_1}) \\ &= \mathbf{t} + (\mathbf{r}_{a_3} - \mathbf{r}_{a_1}) + \exp((\theta_{a_1} + \theta_{a_2} + \theta_{a_3})\tilde{\mathbf{s}}_a)(\mathbf{r}_{b_2} - \mathbf{r}_{b_1})\end{aligned}\quad (20)$$

Taking dot product of  $\mathbf{s}_a$  on both sides of Equation (20) to eliminate  $\theta_{a_1} + \theta_{a_2}$  and  $\theta_{a_1}$ , the equation having the only parameter  $\theta_{b_1}$  can be obtained as

$$A \sin \theta_{b_1} + B \cos \theta_{b_1} = C, \quad (21)$$

where

$$\begin{aligned}A &= (\exp((\theta_{a_1} + \theta_{a_2} + \theta_{a_3})\tilde{\mathbf{s}}_a)(\mathbf{s}_b \times (\mathbf{r}_{b_2} - \mathbf{r}_{b_1})))^T \mathbf{s}_a, \\ B &= (\exp((\theta_{a_1} + \theta_{a_2} + \theta_{a_3})\tilde{\mathbf{s}}_a)(\mathbf{r}_{b_2} - \mathbf{r}_{b_1} - \mathbf{r}_{b_2}^T \mathbf{s}_b \mathbf{s}_b + \mathbf{r}_{b_1}^T \mathbf{s}_b \mathbf{s}_b))^T \mathbf{s}_a, \\ C &= (\mathbf{t} + (\mathbf{r}_{a_3} - \mathbf{r}_{a_1} - \mathbf{r}_{a_3}^T \mathbf{s}_a \mathbf{s}_a + \mathbf{r}_{a_1}^T \mathbf{s}_a \mathbf{s}_a))^T \mathbf{s}_a.\end{aligned}$$

In Equation (21),  $A$ ,  $B$ , and  $C$  are known quantities. Thus,  $\theta_{b_1}$  can be solved as follows using the half-tangent formula

$$\theta_{b_1} = 2\arctan\left(\frac{A \pm \sqrt{A^2 + B^2 - C^2}}{B + C}\right). \quad (22)$$

We substitute the obtained  $\theta_{b_1}$  into Equation (20) to solve  $\theta_{a_1} + \theta_{a_2}$  and  $\theta_{a_1}$ ,

$$\begin{aligned}&\exp((\theta_{a_1} + \theta_{a_2})\tilde{\mathbf{s}}_a)(\mathbf{r}_{a_3} - \mathbf{r}_{a_2}) + \exp(\theta_{a_1}\tilde{\mathbf{s}}_a)(\mathbf{r}_{a_2} - \mathbf{r}_{a_1}) \\ &= \mathbf{t} + (\mathbf{r}_{a_3} - \mathbf{r}_{a_1}) - \exp((\theta_{a_1} + \theta_{a_2} + \theta_{a_3})\tilde{\mathbf{s}}_a)(\exp(\theta_{b_1}\tilde{\mathbf{s}}_b) - \mathbf{E}_3)(\mathbf{r}_{b_2} - \mathbf{r}_{b_1})\end{aligned}\quad (23)$$

In order to solve  $\theta_{a_1} + \theta_{a_2}$  and  $\theta_{a_1}$ , the following two equations are obtained by using Euler formula and taking variable substitutions  $\theta_1 = \theta_{a_1} + \theta_{a_2}$  and  $\theta_2 = \theta_{a_1}$ ,

$$A_1 \sin \theta_1 + B_1 \cos \theta_1 + C \sin \theta_2 = D_1, \quad (24)$$

$$A_2 \sin \theta_1 + B_2 \cos \theta_1 + C \cos \theta_2 = D_2, \quad (25)$$

where

$$\begin{aligned}A_1 &= (\mathbf{s}_a \times (\mathbf{r}_{a_3} - \mathbf{r}_{a_2}))^T (\mathbf{s}_a \times (\mathbf{r}_{a_2} - \mathbf{r}_{a_1})), \quad B_1 = (\mathbf{r}_{a_3} - \mathbf{r}_{a_2} - \mathbf{r}_{a_3}^T \mathbf{s}_a \mathbf{s}_a + \mathbf{r}_{a_2}^T \mathbf{s}_a \mathbf{s}_a)^T (\mathbf{s}_a \times (\mathbf{r}_{a_2} - \mathbf{r}_{a_1})), \\ C &= |\mathbf{r}_{a_2} - \mathbf{r}_{a_1} - \mathbf{r}_{a_2}^T \mathbf{s}_a \mathbf{s}_a + \mathbf{r}_{a_1}^T \mathbf{s}_a \mathbf{s}_a|^2, \\ D_1 &= \left( \mathbf{t} + (\mathbf{r}_{a_3} - \mathbf{r}_{a_1} - \mathbf{r}_{a_3}^T \mathbf{s}_a \mathbf{s}_a + \mathbf{r}_{a_1}^T \mathbf{s}_a \mathbf{s}_a) \right. \\ &\quad \left. - \exp((\theta_{a_1} + \theta_{a_2} + \theta_{a_3})\tilde{\mathbf{s}}_a)(\exp(\theta_{b_1}\tilde{\mathbf{s}}_b) - \mathbf{E}_3)(\mathbf{r}_{b_2} - \mathbf{r}_{b_1}) \right)^T (\mathbf{s}_a \times (\mathbf{r}_{a_2} - \mathbf{r}_{a_1})), \\ A_2 &= (\mathbf{s}_a \times (\mathbf{r}_{a_3} - \mathbf{r}_{a_2}))^T (\mathbf{r}_{a_2} - \mathbf{r}_{a_1} - \mathbf{r}_{a_2}^T \mathbf{s}_a \mathbf{s}_a + \mathbf{r}_{a_1}^T \mathbf{s}_a \mathbf{s}_a), \\ B_2 &= (\mathbf{r}_{a_3} - \mathbf{r}_{a_2} - \mathbf{r}_{a_3}^T \mathbf{s}_a \mathbf{s}_a + \mathbf{r}_{a_2}^T \mathbf{s}_a \mathbf{s}_a)^T (\mathbf{r}_{a_2} - \mathbf{r}_{a_1} - \mathbf{r}_{a_2}^T \mathbf{s}_a \mathbf{s}_a + \mathbf{r}_{a_1}^T \mathbf{s}_a \mathbf{s}_a)\end{aligned}$$



$$D_2 = \begin{pmatrix} \mathbf{t} + (\mathbf{r}_{a_3} - \mathbf{r}_{a_1} - \mathbf{r}_{a_3}^T \mathbf{s}_a \mathbf{s}_a + \mathbf{r}_{a_1}^T \mathbf{s}_a \mathbf{s}_a) \\ -\exp((\theta_{a_1} + \theta_{a_2} + \theta_{a_3}) \tilde{\mathbf{s}}_a) (\exp(\theta_{b_1} \tilde{\mathbf{s}}_b) - \mathbf{E}_3) (\mathbf{r}_{b_2} - \mathbf{r}_{b_1}) \end{pmatrix}^T (\mathbf{r}_{a_2} - \mathbf{r}_{a_1} - \mathbf{r}_{a_2}^T \mathbf{s}_a \mathbf{s}_a + \mathbf{r}_{a_1}^T \mathbf{s}_a \mathbf{s}_a)$$

Combining these two equations and using the half-tangent formula leads to a quartic equation of  $\tan \frac{\theta_1}{2}$  as follows:

$$\begin{aligned} & (B_1^2 + B_2^2 + D_1^2 + D_2^2 - C^2 + 2B_1D_1 + 2B_2D_2) \tan^4 \frac{\theta_1}{2} \\ & - 4(A_1B_1 + A_2B_2 + A_1D_1 + A_2D_2) \tan^3 \frac{\theta_1}{2} \\ & + 2(2A_1^2 + 2A_2^2 + D_1^2 + D_2^2 - C^2 - B_1^2 - B_2^2) \tan^2 \frac{\theta_1}{2} \\ & + 4(A_1B_1 + A_2B_2 - A_1D_1 - A_2D_2) \tan \frac{\theta_1}{2} \\ & + (B_1^2 + B_2^2 + D_1^2 + D_2^2 - C^2 - 2B_1D_1 - 2B_2D_2) = 0 \end{aligned} \quad (26)$$

As  $A_i, B_i, C, D_i$  ( $i = 1, 2$ ) are known quantities,  $\theta_{a_1} + \theta_{a_2}$  can be solved using the quartic formula. Here, we do not list the detailed results due to space limitations. Substituting the analytical solution of  $\theta_{a_1} + \theta_{a_2}$  into Equations (24) and (25) leads to the solution of  $\theta_{a_1}$  as follows:

$$\theta_{a_1} = \arctan 2 \left( \frac{\frac{D_1}{C} - \frac{A_1}{C} \sin(\theta_{a_1} + \theta_{a_2}) - \frac{B_1}{C} \cos(\theta_{a_1} + \theta_{a_2})}{\frac{D_2}{C} - \frac{A_2}{C} \sin(\theta_{a_1} + \theta_{a_2}) - \frac{B_2}{C} \cos(\theta_{a_1} + \theta_{a_2})} \right) \quad (27)$$

Consequently, using the displacement model based upon finite screw and the procedures in Section 3, the forward and inverse kinematics of the two SRs are all solved, which shows the validity of the proposed new method.

## 5. Matlab Simulation

Using finite screw as mathematical tool, the displacement models of  $P_1P_2P_3R_aR_b$  and  $R_aR_aR_aR_bR_b$  robots are easily formulated, and the solutions for forward and inverse kinematics of these two SRs are systematically derived in an analytical manner. In this section, the obtained analytical solutions will be verified through Matlab simulation, which leads to the correctness of the proposed method.

### 5.1. $P_1P_2P_3R_aR_b$

As shown in Figure 2,  $P_1P_2P_3R_aR_b$  is the basic and simplest three-translational and two-rotational SR. Using Matlab software R2023b, the inverse kinematic solutions of the five joint parameters obtained from the derivations in Section 4.1 are programmed. We arbitrarily set the values of the unit vectors and position vectors of its joints and the pose of end-effector as follows:

$$\begin{aligned} \mathbf{s}_1^T &= (1 \ 0 \ 0)^T, \mathbf{s}_2^T = (0 \ 1 \ 0)^T, \mathbf{s}_3^T = (0 \ 0 \ 1)^T, \\ \mathbf{s}_a^T &= \left( \frac{\sqrt{3}}{3} \ \frac{\sqrt{3}}{3} \ \frac{\sqrt{3}}{3} \right)^T, \mathbf{r}_a^T = (1 \ 1 \ 2)^T, \mathbf{s}_b^T = \left( \frac{\sqrt{2}}{2} \ 0 \ \frac{\sqrt{2}}{2} \right)^T, \\ & \mathbf{r}_b^T = (0 \ 0 \ 4)^T, \\ \mathbf{s}_{SR}^T &= \left( \frac{\sqrt{2}}{2} \ \frac{1}{2} \ \frac{1}{2} \right)^T, \mathbf{r}_{SR}^T = (0 \ 0 \ 3)^T, \theta_{SR} = 2.5717, \tau_{SR} = 1 \end{aligned}$$

The joint parameters can be automatically solved in Matlab as follows:

$$\tau_1 = -1.3719, \tau_2 = 0.5791, \tau_3 = 2.1185, \theta_a = 2.0944, \theta_b = 0.5698$$

Substituting these joint parameters into the forward kinematic program shows that the resultant pose is identical to the given pose ( $\mathbf{s}_{SR}, \mathbf{r}_{SR}, \theta_{SR}, \tau_{SR}$ ). Hence, the analytical solutions in Section 4.1 are verified to be correct.

### 5.2. $R_a R_a R_a R_b R_b$

$R_a R_a R_a R_b R_b$  is a rather complicated SR, as shown in Figure 3. The inverse kinematic solutions of the five joint parameters obtained from the derivations in Section 4.2 are programmed in Matlab software. Similarly, the unit vectors and position vectors of its joints and the pose of end-effector are arbitrarily given values, as follows:

$$\begin{aligned} \mathbf{s}_a^T &= \left( \frac{\sqrt{3}}{3} \quad \frac{\sqrt{3}}{3} \quad \frac{\sqrt{3}}{3} \right)^T, \mathbf{r}_{a_1}^T = (1 \quad 1 \quad 1)^T, \mathbf{r}_{a_2}^T = (1 \quad 1 \quad 2)^T, \mathbf{r}_{a_3}^T = (1 \quad 1 \quad 3)^T \\ \mathbf{s}_b^T &= \left( \frac{\sqrt{2}}{2} \quad 0 \quad \frac{\sqrt{2}}{2} \right)^T, \mathbf{r}_{b_1}^T = (0 \quad 0 \quad 3)^T, \mathbf{r}_{b_2}^T = (0 \quad 0 \quad 4)^T \\ \mathbf{s}_{SR}^T &= \left( \frac{\sqrt{2}}{2} \quad \frac{1}{2} \quad \frac{1}{2} \right)^T, \mathbf{r}_{SR}^T = (2 \quad 1 \quad 2.2)^T, \theta_{SR} = 2.5717, \tau_{SR} = 1 \end{aligned}$$

Matlab can automatically calculate the two sets of joint parameters as

$$\theta_{a_1} = 2.4810, \theta_{a_2} = -0.6874, \theta_{a_3} = 0.3007, \theta_{b_1} = -0.6281, \theta_{b_2} = 1.1980$$

and

$$\theta_{a_1} = 1.7936, \theta_{a_2} = 0.6874, \theta_{a_3} = -0.3867, \theta_{b_1} = -0.6281, \theta_{b_2} = 1.1980$$

Substituting each set of these joint parameters into the forward kinematic program can verify the correctness of the analytical solutions in Section 4.2.

In fact, numerous groups of values of the joint axes and poses of the end-effector are attempted in the inverse kinematic programs of both  $P_1 P_2 P_3 R_a R_b$  and  $R_a R_a R_a R_b R_b$  robots. All the solved joint parameters lead to the given pose in the forward kinematic program. In this way, the correctness of the proposed finite screw method is verified through Matlab simulation. Here, we just list one group of values and solutions for each robot for an example.

## 6. Discussions and Conclusions

Employing finite screw as mathematical tool, this paper presents a new method for displacement modelling. Forward kinematics of the SR can be directly carried out using the formulated displacement equation. Meanwhile, the process for inverse kinematics is also given. Two SRs with three translations and two rotations are given as examples to show the validity of the proposed method. However, it should be pointed out that the detailed computations on solving the inverse kinematics of SRs with more than two rotations are still under investigations by the authors.

The following conclusions are drawn:

- (1) The displacement equation of SR is algebraically formulated through describing displacements generated by SR and its joints employing finite screws;
- (2) The procedures for forward and inverse kinematics by analytically solving the formulated displacement equation are discussed in detail;
- (3)  $P_1 P_2 P_3 R_a R_b$  and  $R_a R_a R_a R_b R_b$  robots are taken as examples to illustrate the proposed finite screw method. The correctness of the obtained solutions is verified by Matlab simulation.

This paper provides a new idea and method for displacement modelling and kinematics of SRs. The proposed method for displacement modelling of SR offers a novel approach, which provides a more accurate and efficient way for displacement modelling, which may have significant implications for various applications. Our study mainly focuses on theoretical analysis and simulation. Though we have demonstrated the effectiveness of our method in these aspects, further experimental validation is needed to fully assess its performance in practical applications.

**Author Contributions:** Conceptualization, F.X. and S.Y.; methodology, S.Y.; software, Z.F. and J.S.; validation, F.X., S.Y. and Q.L.; writing—original draft preparation, F.X. and S.Y.; writing—review and editing, F.X.; visualization, Z.F. and J.S.; supervision, S.Y. and Q.L.; project administration, S.Y. All authors have read and agreed to the published version of the manuscript.

**Funding:** This research work is supported by the National Natural Science Foundation of China (NSFC) under Grants 52305042 and 52205029, the Natural Science Foundation of Tianjin under Grant 23JCQNJC00430, and State Key Laboratory of Robotics and Systems (HIT) under Grant SKLRS-2023-KF-07.

**Data Availability Statement:** The data presented in this study are available on request from the corresponding author.

**Conflicts of Interest:** The authors declare no conflicts of interest. The funders had no role in the design of the study; in the collection, analyses, or interpretation of data; in the writing of the manuscript; or in the decision to publish the results.

## References

1. Yan, S.J.; Ong, S.K.; Nee, A.Y.C. Optimal pass planning for robotic welding of large-dimension joints with deep grooves. *Procedia CIRP* **2016**, *56*, 188–192. [[CrossRef](#)]
2. Curiel, D.; Veiga, F.; Suarez, A.; Villanueva, P.; Aldalur, E. Automatic trajectory determination in automated robotic welding considering weld joint symmetry. *Symmetry* **2023**, *15*, 1776. [[CrossRef](#)]
3. Jia, G.; Huang, H.; Li, B.; Wu, Y.; Cao, Q.; Guo, H. Synthesis of a novel type of metamorphic mechanism module for large scale deployable grasping manipulators. *Mech. Mach. Theory* **2018**, *128*, 544–559. [[CrossRef](#)]
4. Jia, G.; Huang, H.; Wang, S.; Li, B. Type synthesis of plane-symmetric deployable grasping parallel mechanisms using constraint force parallelogram law. *Mech. Mach. Theory* **2021**, *161*, 104330. [[CrossRef](#)]
5. Song, Y.; Kang, X.; Dai, J.S. Instantaneous mobility analysis using the twist space intersection approach for parallel mechanisms. *Mech. Mach. Theory* **2020**, *151*, 103866. [[CrossRef](#)]
6. Huo, X.; Song, Y. Finite motion analysis of parallel mechanisms with parasitic motions based on conformal geometric algebra. *Adv. Appl. Clifford Algebras* **2018**, *28*, 21. [[CrossRef](#)]
7. Huo, X.; Lian, B.; Wang, P.; Song, Y.; Sun, T. Topology and dimension synchronous optimization of 1T2R parallel robots. *Mech. Mach. Theory* **2023**, *187*, 105385. [[CrossRef](#)]
8. Di Gregorio, R. Singularity Analysis of spatial single-DOF mechanisms based on the locations of the instantaneous screw axes. *Mech. Mach. Theory* **2023**, *189*, 105438. [[CrossRef](#)]
9. Hu, B.; Bai, P. Type synthesis of serial kinematic chains with screw type terminal constraints based on an adding joint method. *Mech. Mach. Theory* **2023**, *184*, 105277. [[CrossRef](#)]
10. Song, Y.; Ma, X.; Dai, J.S. A novel 6R metamorphic mechanism with eight motion branches and multiple furcation points. *Mech. Mach. Theory* **2019**, *142*, 103598. [[CrossRef](#)]
11. Sun, T.; Huo, X. Type synthesis of 1T2R parallel mechanisms with parasitic motions. *Mech. Mach. Theory* **2018**, *128*, 412–428. [[CrossRef](#)]
12. Lian, B.; Sun, T.; Song, Y.; Wang, X. Passive and active gravity compensation of horizontally-mounted 3-RPS parallel kinematic machine. *Mech. Mach. Theory* **2016**, *104*, 190–201. [[CrossRef](#)]
13. Feng, H.; Chen, Y.; Dai, J.S.; Gogu, G. Kinematic study of the general plane-symmetric Bricard linkage and its bifurcation variations. *Mech. Mach. Theory* **2017**, *116*, 89–104. [[CrossRef](#)]
14. Shen, F.; Yang, S.; Wang, H.; Dai, J.S. Twist and finite twist analysis of 2UPR-SPR parallel mechanism based upon screw theory. *Mech. Mach. Theory* **2023**, *184*, 105276. [[CrossRef](#)]
15. Wang, K.; Dai, J.S. The dual Euler-Rodrigues formula in various mathematical forms and their intrinsic relations. *Mech. Mach. Theory* **2023**, *181*, 105184. [[CrossRef](#)]
16. Chen, K.; Wang, R.; Niu, Z.; Wang, P.; Sun, T. Topology design and performance optimization of six-limbs 5-DOF parallel machining robots. *Mech. Mach. Theory* **2023**, *185*, 105333. [[CrossRef](#)]
17. Feng, H.; Peng, R.; Ma, J.; Chen, Y. Rigid foldability of generalized triangle twist origami pattern and its derived 6R linkages. *J. Mech. Robot.* **2018**, *10*, 051003. [[CrossRef](#)]
18. Gao, C.; Huang, H.; Li, B.; Jia, G. Design of a truss-shaped deployable grasping mechanism using mobility bifurcation. *Mech. Mach. Theory* **2019**, *139*, 346–358. [[CrossRef](#)]
19. Yang, Q.; Hu, K.; Zhang, Y.; Lian, B.; Sun, T. Design and experiment of multi-locomotion tensegrity mobile robot. *Mech. Mach. Theory* **2024**, *198*, 105671. [[CrossRef](#)]
20. Wang, S.; Huang, H.; Jia, G.; Li, B.; Guo, H.; Liu, R. Design of a novel three-limb deployable mechanism with mobility bifurcation. *Mech. Mach. Theory* **2022**, *172*, 104789. [[CrossRef](#)]
21. Dai, J.S. An historical review of the theoretical development of rigid body displacements from Rodrigues parameters to the finite twist. *Mech. Mach. Theory* **2006**, *41*, 41–52. [[CrossRef](#)]

22. Dai, J.S. Finite displacement screw operators with embedded Chasles' motion. *J. Mech. Robot.* **2012**, *4*, 041002. [[CrossRef](#)]
23. Dai, J.S.; Holland, N.; Kerr, D.R. Finite twist mapping and its application to planar serial manipulators with revolute joints. *Proc. Inst. Mech. Eng. Part C J. Mech. Eng. Sci.* **1995**, *209*, 263–271. [[CrossRef](#)]
24. Ma, Y.; Liu, H.; Zhang, M.; Li, B.; Liu, Q.; Dong, C. Elasto-dynamic performance evaluation of a 6-DOF hybrid polishing robot based on kinematic modeling and CAE technology. *Mech. Mach. Theory* **2022**, *176*, 104983. [[CrossRef](#)]
25. Jin, Y.; Yang, Q.; Liu, X.; Lian, B.; Sun, T. Type synthesis of worm-like planar tensegrity mobile robot. *Mech. Mach. Theory* **2024**, *191*, 105476. [[CrossRef](#)]
26. Sun, T.; Song, Y.; Dong, G.; Lian, B.; Liu, J. Optimal design of a parallel mechanism with three rotational degrees of freedom. *Robot. Comput.-Integr. Manuf.* **2012**, *28*, 500–508. [[CrossRef](#)]
27. Jia, G.; Li, B.; Huang, H.; Zhang, D. Type synthesis of metamorphic mechanisms with scissor-like linkage based on different kinds of connecting pairs. *Mech. Mach. Theory* **2020**, *151*, 103848. [[CrossRef](#)]
28. Sun, T.; Lian, B.; Song, Y.; Feng, L. Elastodynamic optimization of a 5-DoF parallel kinematic machine considering parameter uncertainty. *IEEE/ASME Trans. Mechatron.* **2019**, *24*, 315–325. [[CrossRef](#)]
29. Ding, X.; Yang, Y.; Dai, J.S. Topology and kinematic analysis of color-changing ball. *Mech. Mach. Theory* **2011**, *46*, 67–81. [[CrossRef](#)]
30. Huo, X.; Lian, B.; Wang, P.; Song, Y.; Sun, T. Dynamic identification of a tracking parallel mechanism. *Mech. Mach. Theory* **2021**, *155*, 104091. [[CrossRef](#)]
31. Gan, D.; Dai, J.S.; Dias, J.; Seneviratne, L.D. Variable motion/force transmissibility of a metamorphic parallel mechanism with reconfigurable 3T and 3R motion. *J. Mech. Robot.* **2016**, *8*, 051001. [[CrossRef](#)]
32. Sun, T.; Liu, C.; Lian, B.; Wang, P.; Song, Y. Calibration for precision kinematic control of an articulated serial robot. *IEEE Trans. Ind. Electron.* **2021**, *68*, 6000–6009. [[CrossRef](#)]
33. Kang, R.; Guo, Y.; Chen, L.; Branson, D.T.; Dai, J.S. Design of a pneumatic muscle based continuum robot with embedded tendons. *IEEE/ASME Trans. Mechatron.* **2017**, *22*, 751–761. [[CrossRef](#)]
34. Liu, H.; Dai, J. An approach to carton-folding trajectory planning using dual robotic fingers. *Robot. Auton. Syst.* **2003**, *42*, 47–63. [[CrossRef](#)]
35. Sun, T.; Lian, B.; Song, Y. Stiffness Analysis of a 2-DoF over-constrained RPM with an articulated traveling platform. *Mech. Mach. Theory* **2016**, *96*, 165–178. [[CrossRef](#)]
36. Sun, T.; Wu, H.; Lian, B.; Qi, Y.; Wang, P.; Song, Y. Stiffness modeling, analysis and evaluation of a 5 degree of freedom hybrid manipulator for friction stir welding. *Proc. Inst. Mech. Eng. Part C J. Mech. Eng. Sci.* **2017**, *231*, 4441–4456. [[CrossRef](#)]
37. Tang, G.; Yang, Q.; Lian, B. Design and experimentation of tensegrity jumping robots. *Appl. Sci.* **2024**, *14*, 3947. [[CrossRef](#)]
38. Zhao, J.-S.; Wang, J.-Y.; Chu, F.; Feng, Z.-J.; Dai, J.S. Structure synthesis and statics analysis of a foldable stair. *Mech. Mach. Theory* **2011**, *46*, 998–1015. [[CrossRef](#)]
39. Yan, S.J.; Ong, S.K.; Nee, A.Y.C. Stiffness analysis of parallelogram-type parallel manipulators using a strain energy method. *Robot. Comput.-Integr. Manuf.* **2016**, *37*, 13–22. [[CrossRef](#)]
40. Aimedee, F.; Gogu, G.; Dai, J.S.; Bouzgarrou, C.; Bouton, N. Systematization of morphing in reconfigurable mechanisms. *Mech. Mach. Theory* **2016**, *96*, 215–224. [[CrossRef](#)]
41. Wang, R.; Song, Y.; Dai, J.S. Reconfigurability of the origami-inspired integrated 8R kinematotropic metamorphic mechanism and its evolved 6R and 4R mechanisms. *Mech. Mach. Theory* **2021**, *161*, 104245. [[CrossRef](#)]
42. Yan, S.J.; Ong, S.K.; Nee, A.Y.C. Optimization design of general triglide parallel manipulators. *Adv. Robot.* **2016**, *30*, 1027–1038. [[CrossRef](#)]
43. Dai, J.S.; Jones, J.R. A linear algebraic procedure in obtaining reciprocal screw systems. *J. Robot. Syst.* **2003**, *20*, 401–412. [[CrossRef](#)]
44. Menestrasti, L.; Cannella, F.; Pupilli, M.; Dai, J.S. Large bending behavior of creased paperboard. I. Experimental investigations. *Int. J. Solids Struct.* **2013**, *50*, 3089–3096. [[CrossRef](#)]
45. Hunt, K.H. *Kinematic Geometry of Mechanisms*; Oxford University Press: Oxford, UK, 1978.
46. Qin, Y.; Dai, J.S.; Gogu, G. Multi-furcation in a derivative queer-square mechanism. *Mech. Mach. Theory* **2014**, *81*, 36–53. [[CrossRef](#)]
47. Gan, D.; Liao, Q.; Dai, J.S.; Wei, S.; Seneviratne, L.D. Forward displacement analysis of the general 6–6 Stewart mechanism using Gröbner bases. *Mech. Mach. Theory* **2009**, *44*, 1640–1647. [[CrossRef](#)]
48. Ball, R.S. *A Treatise on the Theory of Screws*; Cambridge University Press: Cambridge, UK, 1900.
49. Hamilton, W.R. *Elements of Quaternions*; Longmans, Green, & Company: London, UK, 1886.
50. Rodriguez Leal, E.; Dai, J.S. From origami to a new class of centralized 3-DOF parallel mechanisms. In Proceedings of the ASME 2007 International Design Engineering Technical Conferences and Computers and Information in Engineering Conference, Las Vegas, NV, USA, 4–7 September 2007; pp. 1183–1193. [[CrossRef](#)]
51. Saglia, J.A.; Tzagarakis, N.G.; Dai, J.S.; Caldwell, D.G. Inverse-kinematics-based control of a redundantly actuated platform for rehabilitation. *Proc. Inst. Mech. Eng. Part I J. Syst. Control Eng.* **2009**, *223*, 53–70. [[CrossRef](#)]
52. Saglia, J.A.; Tzagarakis, N.G.; Dai, J.S.; Caldwell, D.G. Control strategies for ankle rehabilitation using a high performance ankle exerciser. In Proceedings of the 2010 IEEE International Conference on Robotics and Automation, Anchorage, AK, USA, 3–7 May 2010; pp. 2221–2227. [[CrossRef](#)]
53. Kang, X.; Feng, H.; Dai, J.S.; Yu, H. High-order based revelation of bifurcation of novel Schatz-inspired metamorphic mechanisms using screw theory. *Mech. Mach. Theory* **2020**, *152*, 103931. [[CrossRef](#)]

54. Huo, X.; Yang, S.; Lian, B.; Sun, T.; Song, Y. A survey of mathematical tools in topology and performance integrated modeling and design of robotic mechanism. *Chin. J. Mech. Eng.* **2020**, *33*, 62. [[CrossRef](#)]
55. Tang, T.; Fang, H.; Luo, H.; Song, Y.; Zhang, J. Type synthesis, unified kinematic analysis and prototype validation of a family of Exechon inspired parallel mechanisms for 5-axis hybrid kinematic machine tools. *Robot. Comput.-Integr. Manuf.* **2021**, *72*, 102181. [[CrossRef](#)]
56. Tang, T.; Luo, H.; Song, Y.; Fang, H.; Zhang, J. Chebyshev inclusion function based interval kinetostatic modeling and parameter sensitivity analysis for Exechon-like parallel kinematic machines with parameter uncertainties. *Mech. Mach. Theory* **2021**, *157*, 104209. [[CrossRef](#)]
57. Chen, X.; Feng, H.; Ma, J.; Chen, Y. A plane linkage and its tessellation for deployable structure. *Mech. Mach. Theory* **2019**, *142*, 103605. [[CrossRef](#)]
58. Wang, T.; Lin, Y.-H.; Spyrakos-Papastavridis, E.; Xie, S.Q.; Dai, J.S. Stiffness evaluation of a novel ankle rehabilitation exoskeleton with a type-variable constraint. *Mech. Mach. Theory* **2023**, *179*, 105071. [[CrossRef](#)]
59. Chen, Z.; Chen, Q.; Jia, G.; Dai, J.S. Sylvester's dialytic elimination in analysis of a metamorphic mechanism derived from ladybird wings. *Mech. Mach. Theory* **2023**, *179*, 105102. [[CrossRef](#)]
60. Guo, F.; Sun, T.; Wang, P.; Liu, S.; Song, Y. Synchronous design method of stiffness and topology for parallel flexible mechanisms with various joints. *Mech. Mach. Theory* **2023**, *180*, 105137. [[CrossRef](#)]
61. Salerno, M.; Zhang, K.; Menciasci, A.; Dai, J.S. A novel 4-DOFs origami enabled, SMA actuated, robotic end-effector for minimally invasive surgery. In Proceedings of the 2014 IEEE International Conference on Robotics and Automation (ICRA), Hong Kong, China, 31 May–7 June 2014; pp. 2844–2849. [[CrossRef](#)]
62. Yao, L.; Gu, B.; Haung, S.; Wei, G.; Dai, J.S. Mathematical modeling and simulation of the external and internal double circular-arc spiral bevel gears for the nutation drive. *J. Mech. Des.* **2010**, *132*, 021008. [[CrossRef](#)]
63. Huijuan, F.; Jiayao, M.; Yan, C. Rigid folding of generalized waterbomb origami tubes. *J. Mech. Eng.* **2020**, *56*, 143. [[CrossRef](#)]
64. Sun, T.; Song, Y.; Li, Y.; Liu, L. Dimensional synthesis of a 3-DOF parallel manipulator based on dimensionally homogeneous Jacobian matrix. *Sci. China Ser. E Technol. Sci.* **2010**, *53*, 168–174. [[CrossRef](#)]
65. Yao, W.; Dai, J.S. Dexterous manipulation of origami cartons with robotic fingers based on the interactive configuration space. *J. Mech. Des.* **2008**, *130*, 022303. [[CrossRef](#)]
66. Aldalur, E.; Suárez, A.; Curiel, D.; Veiga, F.; Villanueva, P. Intelligent and adaptive system for welding process automation in T-shaped joints. *Metals* **2023**, *13*, 1532. [[CrossRef](#)]
67. Feng, H.; Lv, W.; Ma, J.; Chang, W.; Chen, Y.; Wang, J. Helical structures with switchable and hierarchical chirality. *Appl. Phys. Lett.* **2020**, *116*, 194102. [[CrossRef](#)]
68. Feng, H.; Ma, J.; Chen, Y.; You, Z. Twist of tubular mechanical metamaterials based on waterbomb origami. *Sci. Rep.* **2018**, *8*, 9522. [[CrossRef](#)] [[PubMed](#)]
69. Zhang, K.; Dai, J.S. Screw-system-variation enabled reconfiguration of the Bennett plano-spherical hybrid linkage and its evolved parallel mechanism. *J. Mech. Des.* **2015**, *137*, 062303. [[CrossRef](#)]
70. Zhao, T.S.; Dai, J.S.; Huang, Z. Geometric synthesis of spatial parallel manipulators with fewer than six degrees of freedom. *Proc. Inst. Mech. Eng. Part C J. Mech. Eng. Sci.* **2002**, *216*, 1175–1185. [[CrossRef](#)]
71. Sun, T.; Yang, S.; Huang, T.; Dai, J.S. A way of relating instantaneous and finite screws based on the screw triangle product. *Mech. Mach. Theory* **2017**, *108*, 75–82. [[CrossRef](#)]
72. Song, C.-Y.; Feng, H.; Chen, Y.; Chen, I.-M.; Kang, R. Reconfigurable mechanism generated from the network of Bennett linkages. *Mech. Mach. Theory* **2015**, *88*, 49–62. [[CrossRef](#)]

**Disclaimer/Publisher's Note:** The statements, opinions and data contained in all publications are solely those of the individual author(s) and contributor(s) and not of MDPI and/or the editor(s). MDPI and/or the editor(s) disclaim responsibility for any injury to people or property resulting from any ideas, methods, instructions or products referred to in the content.